



HAL
open science

Boosted Flight Controller for Quadrotor Navigation under disturbances

Yasser Bouzid, Houria Siguerdidjane, Yasmina Bestaoui

► **To cite this version:**

Yasser Bouzid, Houria Siguerdidjane, Yasmina Bestaoui. Boosted Flight Controller for Quadrotor Navigation under disturbances. IFAC 2017 - 20th World Congress of the International Federation of Automatic Control, Jul 2017, Toulouse, France. pp.10293–10298, 10.1016/j.ifacol.2017.08.1490 . hal-01629394

HAL Id: hal-01629394

<https://hal.science/hal-01629394>

Submitted on 27 Mar 2020

HAL is a multi-disciplinary open access archive for the deposit and dissemination of scientific research documents, whether they are published or not. The documents may come from teaching and research institutions in France or abroad, or from public or private research centers.

L'archive ouverte pluridisciplinaire **HAL**, est destinée au dépôt et à la diffusion de documents scientifiques de niveau recherche, publiés ou non, émanant des établissements d'enseignement et de recherche français ou étrangers, des laboratoires publics ou privés.

Boosted Flight Controller for Quadrotor Navigation under disturbances

Y. Bouzid*. H. Siguerdidjane**. Y. Bestaoui*

* *IBISC, Université d'Evry-Val-d'Essonne, Université Paris-Saclay, Evry, France*
(e-mail : *yasseremp@gmail.com, Yasmina.Bestaoui@ufrst.univ-evry.fr*)

***L2S, CentraleSupélec, Université Paris-Saclay, Gif-sur-yvette, France*
(e-mail : *Houria.Siguerdidjane@centralesupelec.fr*)

Abstract: Lightweight Unmanned Aerial Vehicles (UAV) are usually very sensitive to the external disturbances during outdoor experimentations. These adverse conditions make both the dynamic modeling and the control tasks more complex. Thus, it is necessary to employ an efficient control technique with acceptable performance without a complete knowledge of the disturbed model. This is because, in the classic feedback linearization control, the deviations between the model and the real plant may produce poor performance. Throughout the present paper, Dynamic Sliding Mode Control (DSMC) technique is designed to deal with the disturbances and which has never been used for quadrotors. Unlike the existing sliding mode techniques, the designed one uses an input-dependent sliding surface in order to enhance the robustness level of the classical feedback linearization control law. The effectiveness of this approach that ensures 3D trajectory tracking of quadrotor is demonstrated through numerical simulations.

Keywords: UAV, wind gust, nonlinear control, trajectory tracking, dynamic sliding mode control.

1. INTRODUCTION

The popularity of Vertical Take-Off and Landing (VTOL) vehicles stems from their ease of use and mechanical simplicity compared to other small aircraft. However, in outdoor applications, the vehicle is often operating in windy environment. This external disturbance may strongly affect the performance of the closed loop control. Because of the small size, meteorological circumstances can lead to a loss of the stability especially if the autopilot is not designed to deal with such issues. The trajectory tracking of aerial autonomous systems is a serious task whilst atmospheric disturbances bring more challenge. In an attempt to deal with this problem during the flight, a robust controller is required.

Several robust techniques have been proposed treating the problem of trajectory tracking control for the quadrotors. (Raffo et al. 2008) proposed a nonlinear H_∞ controller and backstepping approach in order to stabilize the attitude and to solve the path-tracking problem of the quadrotor respectively. In reference (Nicol et al. 2011), a robust adaptive control is proposed for the attitude stabilization under external disturbances and validated by real time implementation.

The sliding mode based control is well known for its robustness. Therefore, extensions of the applications have been developed. (Madani et al. 2006; Efe 2007) present a sliding mode combined with backstepping technique for the sake of stabilization, regulation and trajectory tracking. A free-model control scheme inspired from the Passivity-Based Sliding Mode Control (PB-SMC) is proposed (Muñoz-Vázquez et al. 2014). Other approaches are applied as for instance: direct adaptive sliding mode controller in presence of parameter uncertainties (Bouadi et al. 2007), integral sliding mode controller (Seghour et al. 2011) and SMC-

neural networks controllers (Dierks et al. 2010). From this brief review, SMC strategy has been applied successfully for many applications and exhibits good tradeoff between the robustness and the control performance. Motivated by these features, we seek to exploit this framework to design a more efficient controller for the navigation of disturbed quadrotor.

The aim of this paper is to improve the robustness level of the traditional feedback linearization control scheme for a 3D tracking control under disturbances. To accomplish the objective, we propose the Dynamic Sliding Mode Control (DSMC) technique. Unlike the classical SMC, the DSMC employs, as sliding surface, the system input. In reference (Sira-Ramirez & Siguerdidjane 1996), a redundant dynamical scheme was proposed for asymptotic stabilization and has shown very promising results with respect to sudden failures in the designed feedback loop. Up to date, at least to our knowledge, no further exploration neither application is exposed by the scientific community showing the effectiveness of the technique. Herein, we try to supplement this study where the input-dependent sliding surface is employed to boost a feedback linearization controller and improve the robustness level with respect to external disturbances. The sliding surface includes an additional effort needed to deal with the disturbances.

The remainder of the paper is organized as follows: Section 2 introduces the dynamics of the quadrotor. A robust controller based on the sliding mode is detailed and applied to the quadrotor in Section 3. In the same section both stability and robustness are highlighted. In Section 4, the controller effectiveness is shown through numerical simulations. Conclusions are provided in the last section.

2. QUADROTOR MATHEMATICAL MODEL

This section briefly presents the dynamic, which describes the UAV's in-flight behavior. From the fundamental principles of dynamics, we model a quad-copter, considering its rigid structure and neglecting some aerodynamic effects (gyroscopic, ground...), for the validation of performance of the control strategy. The system operates in two coordinate frames, the Earth fixed frame and the body fixed frame that lies at the center of gravity of the vehicle. Let $\eta = (\varphi, \theta, \psi)^T \in [-\frac{\pi}{2}, \frac{\pi}{2}[\times] - \frac{\pi}{2}, \frac{\pi}{2}[\times] - \pi, \pi[$ describes the orientation of the aerial vehicle (Roll, Pitch, Yaw) and $\chi = (x, y, z)^T \in \mathbb{R}^3$ denotes its absolute position.

In conditions of flying at low indoor speed, the simplified dynamic model of the vehicle may be written under the general mechanical equation (Bouazid et al. 2016), as follows

$$\bar{M}(q)\ddot{q} + \bar{G}(q, \dot{q}) = \bar{u} \quad (1)$$

where $q = [\chi, \eta]^T$ is the generalized coordinates, $\bar{M} = \bar{M}^T \in \mathbb{R}^{6 \times 6} = \begin{bmatrix} \mathcal{M} & 0 \\ 0 & I \end{bmatrix} > 0$ is composed of the mass, $\mathcal{M} = mI_{3 \times 3}$, and the diagonal inertia matrix $I = \text{diag}(I_x, I_y, I_z)$.

$$\bar{G} \in \mathbb{R}^6 = \begin{bmatrix} 0 \\ 0 \\ mg \\ (I_z - I_y)\dot{\psi}\dot{\theta} + J_r\dot{\theta}\Omega_r \\ (I_x - I_z)\dot{\phi}\dot{\psi} + J_r\dot{\phi}\Omega_r \\ (I_y - I_x)\dot{\phi}\dot{\theta} \end{bmatrix} \quad (2)$$

and

$$\bar{u} \in \mathbb{R}^6 = (u_x u_1, u_y u_1, c_\theta c_\varphi u_1, u_2, u_3, u_4)^T \quad (3)$$

denotes the input vector with m is the mass, g is the gravity acceleration, u_1 is the total thrust of four rotors and $\tau = (u_2, u_3, u_4)^T$ is the control torques. The terms $J_r\dot{\phi}\Omega_r$ and $J_r\dot{\theta}\Omega_r$ denote the propellers gyroscopic effect, J_r denotes the rotors inertia and Ω_r denotes a mixer of rotors speeds.

Remark 1: To simplify the design of the controllers, two virtual inputs u_x, u_y are considered.

$$\begin{cases} u_x = c_\psi s_\theta c_\varphi + s_\psi s_\varphi \\ u_y = s_\psi s_\theta c_\varphi - c_\psi s_\varphi \end{cases} \quad (4)$$

where $s_{(\cdot)}$ and $c_{(\cdot)}$ are abbreviations for $\sin(\cdot)$ and $\cos(\cdot)$ respectively. We can prove that these virtual inputs have to verify the following equality:

$$u_x^2 + u_y^2 + c_\theta^2 c_\varphi^2 = 1 \quad (5)$$

Notice that this model is quite simplified in order to make the implementation easier. However, more accurate models may be found in the literature (see Bouabdallah 2007). In addition, the system operates in presence of external disturbances whose more common one is the wind gust. Thus, in the following, we describe the motion of the vehicle considering a disturbance vector Δ . Then equation (1) becomes

$$\bar{M}(q)\ddot{q} + \bar{G} = u + \Delta \quad (6)$$

where the disturbance vector is,

$$\Delta = [\delta_x, \delta_y, \delta_z, \delta_\varphi, \delta_\theta, \delta_\psi]^T$$

and u is the input vector for the disturbed model. In general, Δ may represent, not only the effect of the wind gust, but also, model inaccuracies, neglected dynamics, etc.

The quadrotor parameters used in this study are displayed in Table 1.

Table 1. Quadrotor parameters .

| | | | |
|----------------------|--------|----------------------|--------|
| $m(\text{kg})$ | 0.429 | $I_y(\text{kg.m}^2)$ | 0.0029 |
| $I_x(\text{kg.m}^2)$ | 0.0022 | $I_z(\text{kg.m}^2)$ | 0.0048 |

3. DYNAMIC SLIDING MODE CONTROLLER

3.1. Feedback linearization controller

Consider the mechanical full-actuated nominal system

$$\bar{M}(q)\ddot{q} + \bar{G}(q, \dot{q}) = \bar{u} \quad (7)$$

with $q \in D^n \subset \mathbb{R}^n$ denotes the generalized coordinates, $\bar{u} \in \mathbb{R}^n$ is the input vector, $\bar{G}(q, \dot{q}) \in \mathbb{R}^n$ represents a nonlinear n -dimensional vector function and $\bar{M}(q) \in \mathbb{R}^{n \times n}$ denotes a diagonal inertial matrix. In terms of the tracking errors, $e = q - q_r$, model (7) may be written as

$$\bar{M}(e)(\ddot{e} + \ddot{q}_r) + \bar{G}(e, \dot{e}) = \bar{u} \quad (8)$$

where q_r denotes the reference trajectories vector.

Assuming that a smooth feedback controller has been designed in such a way that all the trajectories of closed loop system (8) converge toward the origin. This stabilizing feedback linearization controller is explicitly given by

$$\bar{u} = \zeta(e, \dot{e}) = \bar{M}(e)(v + \ddot{q}_r) + \bar{G}(e, \dot{e}) \quad (9)$$

where

$$v = -K_1 e - K_2 \dot{e} \quad (10)$$

$K_1 > 0, K_2 > 0$ are two positive definite diagonal matrices.

3.2. Stability and robustness analysis

Often, the process modeling involves simplifying assumptions (neglecting some phenomena, considering specific operation modes...). This leads to a mismatch between the real plant and the model. Furthermore, the system is constantly subjected to external disturbances especially the wind gust. Unfortunately, classic feedback controller (9) exhibits poor robustness capabilities to overcome such issues. Moreover, this type of classic controller proceeds by the cancelation of the nonlinearities, which may be changed under the environment effects. So, then, this makes the controller not recommended for highly nonlinear systems as the VTOL vehicles. Nevertheless, we attempt to analyze its robustness level providing the conditions for the stability of the disturbed model. Therefore, through the remainder of this paper, we shall assume disturbed model (6). Commonly, the term Δ is totally unknown but it is supposed to be bounded, $\|\Delta(e, \dot{e})\| \leq d$ where d a positive constant but not very large in such a way the quadrotor remains controllable under disturbances. The state space representation of system (6) is

$$\begin{cases} \dot{e}_1 = e_2 \\ \dot{e}_2 = \bar{M}(e)^{-1}(u - \bar{G}(e, \dot{e})) - \ddot{q}_r + \bar{M}(e)^{-1}\Delta(e, \dot{e}) \end{cases} \quad (11)$$

with $\epsilon = (e_1, e_2)^T = (e, \dot{e})^T$

By using control input vector (9) ($u = \bar{u}$), the closed loop is then written as

$$\begin{cases} \dot{e}_1 = e_2 \\ \dot{e}_2 = -K_1 e - K_2 \dot{e} + \bar{M}(e)^{-1}\Delta(e, \dot{e}) \end{cases} \quad (12)$$

Naturally, system (12) is divided into a nominal one

$$\dot{e} = \vartheta(\epsilon) \quad (13)$$

and additive term

$$\begin{aligned} \theta(\epsilon) &= [0, \bar{M}(e)^{-1} \Delta(e, \dot{e})]^T: D_\epsilon \subset \mathbb{R}^{2n} \rightarrow \mathbb{R}^{2n} \text{ that is} \\ \dot{\epsilon} &= \vartheta(\epsilon) + \theta(\epsilon) \end{aligned} \quad (14)$$

where $\vartheta: D_\epsilon \subset \mathbb{R}^{2n} \rightarrow \mathbb{R}^{2n}$ is a $2n$ -dimensional vector functions sufficiently smooth.

Assuming that the exponential stable equilibrium of nominal system (13) has been established as following:

$$\begin{aligned} \text{Let } V \text{ be a Lyapunov function that satisfies:} \\ \sigma_1 \|\epsilon\|^2 \leq V \leq \sigma_2 \|\epsilon\|^2 \end{aligned} \quad (15)$$

$$\dot{V} \leq -\sigma_3 \|\epsilon\|^2 \quad (16)$$

with

$$\|\nabla V\| \leq \sigma_4 \|\epsilon\| \quad (17)$$

for all $\epsilon \in D_\epsilon$ and $\sigma_i > 0, i = 1, \dots, 4$.

Assuming that $\theta(\epsilon)$, in a bounded neighborhood of the origin, satisfies

$$\|\theta(\epsilon)\| \leq \sigma_5 \|\epsilon\| \quad (18)$$

with $\sigma_5 > 0$.

Now, let us use V , as a candidate Lyapunov function for system (14), to check the robustness of stability in presence of disturbance. The first time derivative of V along (14) gives

$$\dot{V} = \nabla V^T \vartheta(\epsilon) + \nabla V^T \theta(\epsilon) \quad (19)$$

Inequalities (16), (17) and (18) lead to

$$\begin{aligned} \dot{V} &\leq -\sigma_3 \|\epsilon\|^2 + \|\nabla V\| \|\theta(\epsilon)\| \\ &\leq -\sigma_3 \|\epsilon\|^2 + \sigma_4 \sigma_5 \|\epsilon\|^2 \end{aligned} \quad (20)$$

Then the origin is exponentially stable equilibrium if

$$\sigma_5 \leq \frac{\sigma_3}{\sigma_4} \quad (21)$$

In other words: σ_5 has to be small enough. This result is summarized by the following theorem.

Theorem 1: Assuming that: system (13) has the origin as exponential stable equilibrium, the Lyapunov function, $V: D_\epsilon \rightarrow \mathbb{R}^+$ satisfies inequalities (15) - (17) and the disturbance term satisfies condition (18). Then, if (21) holds, the origin of (14) is exponentially stable.

This result is qualitative because the above proof is done without expliciting the knowledge of the Lyapunov function. It is worthwhile to quantify the candidate Lyapunov function and the adequate parameters, $\sigma_i, i = 1, \dots, 5$ that verify equations (15) - (17). Therefore, if

$$V(\epsilon) = \frac{1}{2} \epsilon^T P \epsilon \quad (22)$$

where $P = \begin{bmatrix} p_1 & p_2 \\ p_2 & p_3 \end{bmatrix}$ is a positive definite symmetric matrix of dimension $2n \times 2n$. Notice that

$$\frac{1}{2} \min(\lambda_i) \epsilon^T \epsilon \leq V(\epsilon) \leq \frac{1}{2} \max(\lambda_i) \epsilon^T \epsilon \quad (23)$$

This implies that $\sigma_1 = \min(\lambda_i)$ and $\sigma_2 = \max(\lambda_i)$ where $\lambda_i, i = 1, \dots, 2n$ denotes the eigenvalues of matrix P

The first time derivative of V along (13) gives

$$\begin{aligned} \dot{V}(\epsilon) &= -e_1^T p_2 K_1 e_1 + e_2^T (p_2 - p_3 K_2) e_2 + \\ &\quad e_1^T (p_1 - p_2 K_2 - p_3 K_1) e_2 \end{aligned} \quad (24)$$

Chosen $\sigma_3 = 1$, leads to:

$$\begin{cases} p_1 = K_2^{-1} - K_2^{-1} K_1 + K_1^{-1} K_2 \\ p_2 = K_1^{-1} \\ p_3 = K_1^{-1} K_2^{-1} - K_2^{-1} \end{cases} \quad (25)$$

Matrices p_1, p_2 and p_3 are diagonal and of dimension $n \times n$. From (22), we have

$$\nabla V = P \epsilon$$

That leads to

$$\|\nabla V\| \leq \|P\| \|\epsilon\| \leq \sqrt{2n} \max(\lambda_i) \|\epsilon\|$$

So, in order to satisfy condition (17), we take: $\sigma_4 = \sqrt{2n} \max(\lambda_i), i = 1, \dots, 2n$. Then, the origin of closed loop system (14) is exponentially stable if $\sigma_5 \leq \frac{1}{\sqrt{2n} \max(\lambda_i)}$.

Theorem 2: Let a quadratic Lyapunov function (22), where P is given by (25) that has the eigenvalues $\lambda_i, i = 1, \dots, 2n$. If $\sigma_5 \leq \frac{1}{\sqrt{2n} \max(\lambda_i)}, i = 1, \dots, 2n$ then the origin of system (14) is exponentially stable.

Theorem 1 and Theorem 2 demonstrate the robustness of the stability of this classic controller. However, this is true for very restrictive conditions (Lipschitz disturbance) with small tilt factor σ_5 that shows the sensitivity of the controller at the origin. Therefore, we stress to design a novel controller that improves the robustness level.

3.3. Dynamic sliding mode controller design

Motivated by the limitation of the feedback linearization control to overcome the disturbances, we propose to design a DSMC technique for 3D trajectory tracking of quadrotors under disturbances. Therefore, we consider a supplementary control input, $u = \bar{u} + \delta u$, to reduce the mismatch between the outputs of the plant in the real world and the nominal model. Therefore, system (11) becomes

$$\begin{cases} \dot{e}_1 = e_2 \\ \dot{e}_2 = \bar{M}(e)^{-1} (\bar{u} - \bar{G}(e, \dot{e})) - \ddot{q}_r + \bar{M}(e)^{-1} \delta u + \bar{M}(e)^{-1} \Delta(e, \dot{e}) \end{cases}$$

Generally, to design a sliding mode based control scheme, a surface defined in the state space as a linear form is considered. Contrary to this common case, a surface vector, $S(\epsilon, u) = [s_1, \dots, s_n]^T$, is defined as

$$S(\epsilon, u) = u - \bar{u}(\epsilon) = \delta u(\epsilon, u) \quad (26)$$

where $\delta u(\epsilon, u)$ represents the additional effort from the nominal system to the disturbed one. Such sliding surface has the interpretation that any mismatch between the model and the plant yields a deviation in the input signal. If a control law drives the trajectories such that $S = 0$ holds true, then the disturbance quantity is totally rejected and the tracking errors converge toward the origin.

Considering a positive definite Lyapunov candidate function

$$V = \frac{1}{2} S^T(\epsilon, u) S(\epsilon, u) \quad (27)$$

The first time derivative is

$$\dot{V} = S^T(\epsilon, u) \dot{S}(\epsilon, u) \quad (28)$$

Obviously, the reachability condition of sliding mode control is ensured if \dot{V} is negative definite. In the following, a discontinuous dynamics are introduced by the differential equation

$$\dot{S} = -W \gamma(S(\epsilon, u)) = -W \gamma(\delta u) \quad (29)$$

where W is an arbitrary strictly positive diagonal matrix and $\gamma(\cdot)$ is an operator acting on all the components of the surfaces vector. It is defined for one component by

$$\begin{cases} \gamma(a) < 0 & \text{if } a < 0 \\ \gamma(a) = 0 & \text{if } a = 0 \\ \gamma(a) > 0 & \text{if } a > 0 \end{cases} \quad (30)$$

For example we propose the hyperbolic tangent ($\gamma(a) = \tanh(a)$).

Notice that the trajectories of the components, $s_i(\epsilon, u)$ $i = 1, \dots, n$, of equation (29), independently satisfy the reachability condition, $s_i(\epsilon, u) = 0$, in bounded time t_i , $i = 1, \dots, n$. Using equations (26) and (29) leads down to a dynamical sliding mode controller

$$\dot{S}(\epsilon, u) = \dot{u} - \ddot{u} = -W\gamma(S(\epsilon, u)) \quad (31)$$

Using equation (9), we obtain

$$\dot{S}(\epsilon, u) = \dot{u} - \zeta(e, \dot{e}) = -W\gamma(S(\epsilon, u)) \quad (32)$$

This implies that

$$\dot{u} = -W\gamma(S(\epsilon, u)) + \zeta(e, \dot{e}) \quad (33)$$

with

$$\zeta(e, \dot{e}) = \bar{M}(e)(v + \dot{q}_r) + \bar{G}(e, \dot{e})$$

Equation (33) is a time-varying nonlinear first order differential equation for the control input vector with a switching term. Finally, by straightforward integration, it comes that

$$u = -\int_0^t (W\gamma(S(\epsilon, u)) - \zeta(e, \dot{e})) d\tau + u(0) \quad (34)$$

This new controller, as the classic sliding mode controller, is highly insensitive to external perturbation and to modeling errors. In view of this new formulation, the scheme thus operates as a parallel feedback with high gain loop that enforces the basic smooth feedback linearization control. If the smooth portion has robustness capabilities with respect to certain class of perturbations, the proposed controller that involves, in addition, an integral part has very high robustness features and performance. The integral term plays a compensator role. For this reason, the matrix W needs to be carefully tuned according to the boundaries of the disturbance. This controller is depicted in the block diagram of Fig. 1.

Remark 2: The DSMC may boost the robustness capabilities of any other feedback controller. So, instead of the use of the feedback linearization, we can use the backstepping controller, SMC, etc.

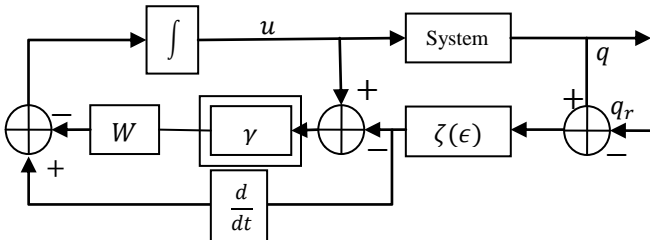


Fig. 1. DSMC diagram.

3.4. Quadrotor application

This section shows how the proposed approach can be applied to the quadrotor in order to ensure the tracking of 3D

reference trajectory. The control structure in Fig. 2 is herein based on the decomposition into two sub-systems. The first one concerns the translation control (outer loop) whilst the second one is for the rotation control (inner loop). Through the virtual control efforts u_x and u_y , the states x and y are controlled to allow the system to reach their references x_r and y_r respectively and provide the reference trajectories (φ_r, θ_r) for the pitch and the roll angles (attitude control) using equation (35). These latter are controlled using u_2 and u_3 respectively. The altitude is controlled by u_1 and the yaw angle is controlled by u_4 in order to track the desired altitude z_r and yaw Ψ_r respectively. The control architecture is shown in Fig. 2. Using equation (4), the roll and pitch reference trajectories are computed through the following equations

$$\begin{cases} \varphi_r = \arcsin(u_x \sin \Psi_r - u_y \cos \Psi_r) \\ \theta_r = \arcsin\left(\frac{u_x \cos \Psi_r + u_y \sin \Psi_r}{\cos \varphi_r}\right) \end{cases} \quad (35)$$

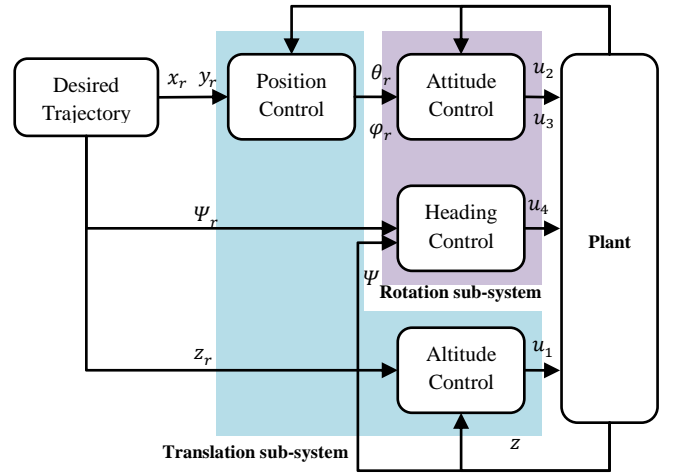


Fig. 2. Quadrotor control architecture.

Previously, we have considered that the UAV system is subject to external disturbances. This is a very motivating reason and it is typical example to check the robustness level of DSMC. First of all, a state-feedback is used. Then, a dynamic sliding mode is involved to provide more robustness with respect to the disturbances by applying the discontinuous operator on each component of the vector S .

4. NUMERICAL SIMULATION

Since we have completed the equations of motion describing the dynamics of the system and the equations of the control laws, we design a Matlab simulation environment in order to check the effectiveness of the DSMC. We have to check the robustness of our controller versus the classic feedback linearization controller. To this end, two scenarios are proposed. In the first scenario, we consider as an example an instantaneous external disturbance that acts only on the altitude dynamic between the intervals of time [8, 10] and [15, 17] seconds. Then a persistent one is considered during the flight of the vehicle. The external disturbance is supposed to be a gust of wind where its profile (velocity) is depicted in Fig. 3 and Fig. 6 using real data. Using the same control

parameters ($K_1 = 5.I_{6 \times 6}$ and $K_2 = 6.I_{6 \times 6}$ with $W=I_{6 \times 6}$), comparative curves are depicted in Fig. 3-Fig. 8 between the classic feedback linearization controller and the DSMC.

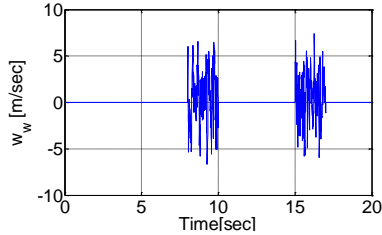


Fig. 3. Instantaneous disturbance profile.

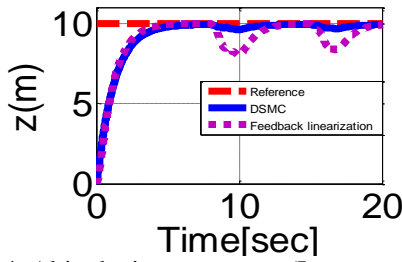


Fig. 4. Altitude time responses (Instantaneous disturbance).

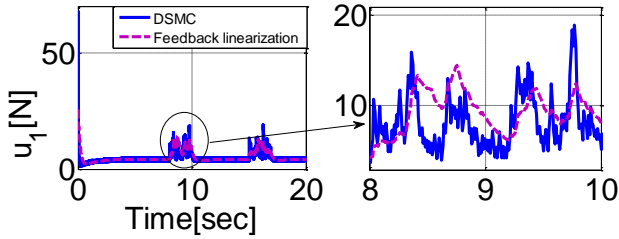


Fig. 5. Thrust signals (instantaneous disturbance).

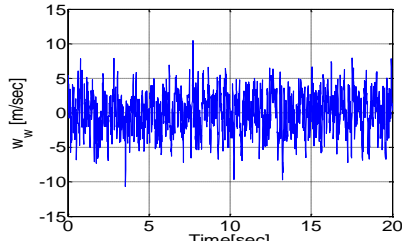


Fig. 6. Persistent disturbance.

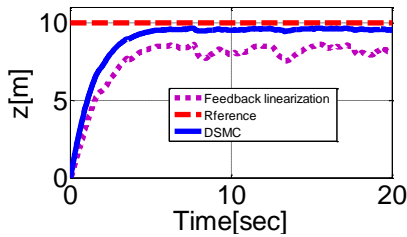


Fig. 7. Altitude time responses (Persistent disturbance).

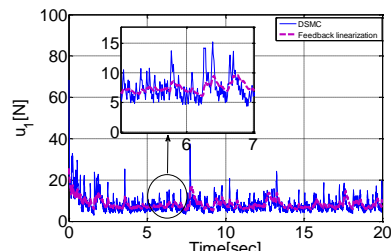


Fig. 8. Thrust signals (Persistent disturbance).

In both cases, the proposed controller based on DSMC exhibits superior performance in terms of accuracy and rapidity. As it may be observed in Fig. 4, the instantaneous perturbation is rejected so its effect is almost totally canceled while the vehicle is clearly influenced using the classic feedback linearization controller. During the persistent perturbation, a significant steady state error appears in Fig. 7 for the feedback linearization controller whilst a very small one is shown for the dynamic sliding mode controller. These results prove the poor capabilities of the feedback linearization controller to tackle the effect of the wind gust compared to those of the boosted controller. However, the control signals are smoother in the case of feedback linearization (see Fig. 5 and Fig. 8). This is due to the switching function (30) employed by DSMC.

In the second case, we seek to show the robustness level of both techniques. Then, a 3D circular trajectory is chosen. For given control parameters, we can check the limits of the robustness by increasing the magnitude of the perturbation. By using the same control parameters, the classical feedback ensures the stability of the system until a perturbation of 5.6908 N (during 5-8 seconds). After this value the system becomes unstable (see Fig. 12). For the same settings and for a perturbation of 6 N, our proposed controller still ensures the stability of the quadrotor. The control parameters of the integral term are $W = \text{diag}(10.5, 1, 0, 0, 1, 0)$. The obtained results are depicted in Fig. 9, Fig. 10 and Fig. 11

From Fig. 9 and Fig. 10, we observe that the vehicle tracks the reference trajectory with very good accuracy. During the application of the perturbation, the controller exhibits a good level of robustness and the effect of the perturbation vanishes after the eighth seconds. As shown in Fig. 11, the control inputs are bounded. However, chattering appears during the application of the perturbation, which is reasonable since the control law include a switching part that reacts at this stage only.

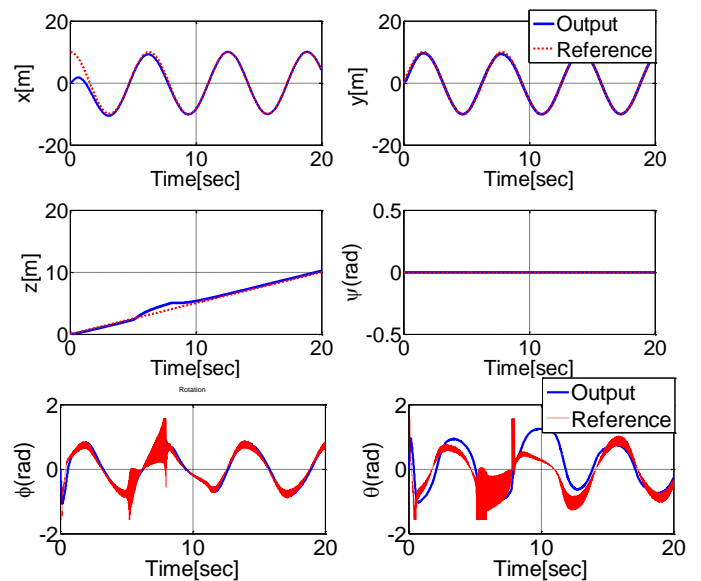


Fig. 9. Overall outputs time responses (DSMC).

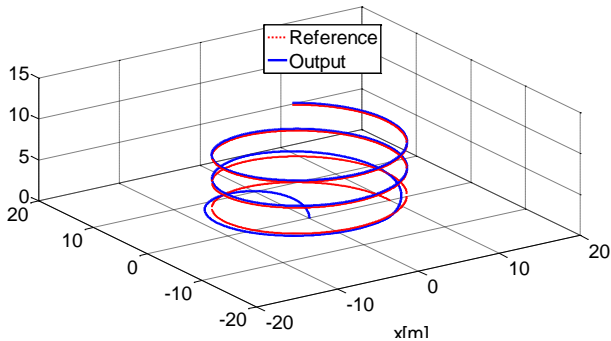


Fig. 10. 3D trajectory (DSMC).

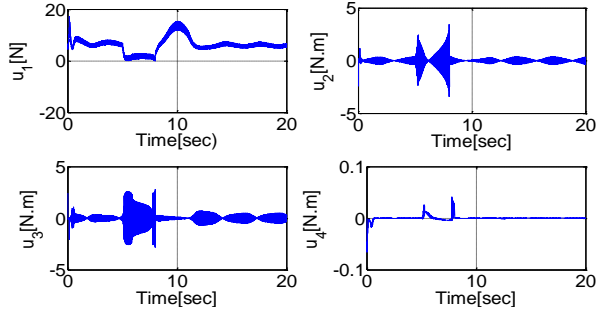


Fig. 11. Input signals (DSMC).

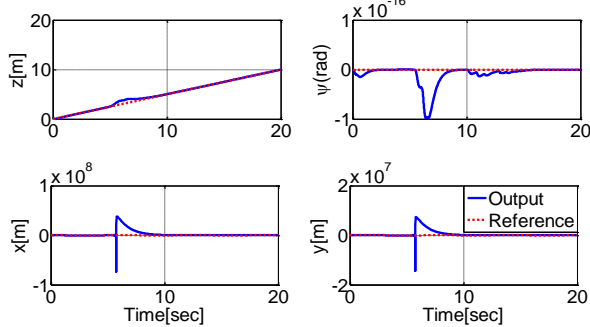


Fig. 12. Outputs time responses (classic feedback).

Finally, at the same conditions, we compare the performance of the DSMC with some other classic published techniques such as the backstepping (BS) control and sliding mode control (Bouabdellah, 2007). Thus, we consider the previous circular trajectory. During the flight, the quadrotor is subjected to persistent wind along the three axes. For a significant comparison we employ the Integral Square Error ($ISE = \int_{t_0}^{t_f} (e_x^2(t) + e_y^2(t) + e_z^2(t)) dt$), the Maximal Absolute Error ($MAE = \max(|e_x|, |e_y|, |e_z|)$) and the consumed energy ($ISCI = \int_{t_0}^{t_f} u_1(t) dt$) as metrics of comparison. The obtained results are depicted in Table 2.

Table 2. Quadrotor parameters.

| | Feedback linearization | SMC | Backstepping | DSMC |
|------|------------------------|---------|--------------|--------|
| ISE | 0.139 | 0.065 | 0.028 | 0.038 |
| MAE | 0.172 | 0.069 | 0.072 | 0.058 |
| ISCI | 678.39 | 2713.72 | 675.04 | 665.35 |

Clearly, from Table 2, the DSMC presents a good compromise between the accuracy and the consumed energy compared to the other techniques with a damped time response. Moreover, the DSMC may employ the input signals

provided by the backstepping technique in order to improve once again the performances.

5. CONCLUSION

The simulations carried out justify the claims, i.e. the proposed DSMC controller performs very well in presence of external disturbances compared to the feedback linearization controller. The results are obtained with a vertical flight and 3D circular trajectory and found to be very accurate. These results are attributed to the robustness property of the proposed dynamic sliding mode controller. The main contributions of this work is a boosted control schema applied to the quadrotor based on the dynamic sliding mode strategy that acts without accurate knowledge about the perturbation.

REFERENCES

- Bouabdellah, S. (2007). *Design and control of quadrotors with application to autonomous flying*. PhD thesis, Laboratoire de systèmes autonomes, École polytechnique fédérale de lausanne.
- Bouadi, H., Bouchoucha, M., and Tadjine, M. (2007). Modelling and stabilizing control laws design based on backstepping for an uav type-quadrotor. *6th IFAC Symposium on Intelligent Autonomous Vehicle, IFAC Proceedings, Volumes*, vol. 40, no. 15, pp. 245–250.
- Bouzid, Y., Siguerdidjane, H., Bestaoui, Y., Zareb, M., 2016. Energy Based 3D Autopilot for VTOL UAV Under Guidance & Navigation Constraints. *J Intell Robot Syst* 1–22. doi:10.1007/s10846-016-0441-1.
- Dierks, T. and Jagannathan, S. (2010). Output Feedback Control of a Quadrotor UAV Using Neural Networks. *IEEE Transactions on Neural Networks*, vol. 21, n° 11.
- Efe, M. O. (2007). Robust low altitude behavior control of a quadrotor rotorcraft through sliding modes. In *Mediterranean Conference on Control Automation, 2007. MED '07*, pp. 1–6.
- Madani, T. and Benallegue, A. (2006). Backstepping Sliding Mode Control Applied to a Miniature Quadrotor Flying Robot. In *IECON- 32nd Annual Conference on IEEE Industrial Electronics*, 2006, pp. 700–705.
- Muñoz-Vázquez, A. J., Parra-Vega, V., Sánchez-Orta A., García, O. and Izaguirre-Espinoza, C. (2014). Attitude tracking control of a quadrotor based on absolutely continuous fractional integral sliding modes. In *2014 IEEE Conference on Control Applications (CCA)*, pp. 717–722.
- Nicol, C., Macnab, C. J. B. and Ramirez-Serrano, A. (2011). Robust adaptive control of a quadrotor helicopter. *Mechatronics*, vol. 21, no. 6, pp. 927–938.
- Raffo, G. V., Ortega, M. G. and Rubio, F. R. (2008). Backstepping/nonlinear H_∞ control for path tracking of a quadrotor unmanned aerial vehicle. In *2008 American Control Conference*, pp. 3356–3361.
- Seghour, S., Bouchoucha, M., and Osmani, H. (2011). From Integral backstepping to integral sliding mode attitude stabilization of a quadrotor system: Real time implementation on an embedded control system based on a dsPIC. *in IEEE International Conference on Mechatronics (ICM)*, pp. 154–161.
- Sira-Ramirez, H., Siguerdidjane, H.B. (1996). A redundant dynamical sliding mode control scheme for an asymptotic space vehicle stabilization. *Int. J. Control*, Vol. 65, No. 6, pp. 901–912.